Title

Stable-isotope and solute-chemistry approaches to flow characterization in a forested tropical watershed, Luquillo Mountains, Puerto Rico

Authors

Scholl, Martha A
Shanley, James B
Murphy, Sheila F
et al.

Publication Date

2015-12-01

DOI

10.1016/j.apgeochem.2015.03.008

Peer reviewed

Applied Geochemistry xxx (2015) xxx–xxx

Contents lists available at ScienceDirect

Applied Geochemistry

journal homepage: www.elsevier.com/locate/apgeochem

Stable-isotope and solute-chemistry approaches to flow characterization in a forested tropical watershed, Luquillo Mountains, Puerto Rico

Martha A. Scholl [a,*], James B. Shanley [b], Sheila F. Murphy [c], Jane K. Willenbring [d], Marcie Occhi [d,e], Grizelle González [f]

[a] U.S. Geological Survey, National Research Program, Reston, VA, United States
[b] U.S. Geological Survey, New Hampshire/Vermont Water Science Center, Montpelier, VT, United States
[c] U.S. Geological Survey, National Research Program, Boulder, CO, United States
[d] University of Pennsylvania, Department of Earth and Environmental Science, Philadelphia, PA, United States
[e] Virginia Department of Mines, Minerals and Energy, Charlottesville, VA, United States
[f] U.S.D.A. Forest Service, International Institute of Tropical Forestry, Río Piedras, PR, United States

ARTICLE INFO

Article history:
Available online xxxx

ABSTRACT

The prospect of changing climate has led to uncertainty about the resilience of forested mountain watersheds in the tropics. In watersheds where frequent, high rainfall provides ample runoff, we often lack understanding of how the system will respond under conditions of decreased rainfall or drought. Factors that govern water supply, such as recharge rates and groundwater storage capacity, may be poorly quantified. This paper describes 8-year data sets of water stable isotope composition (δ^2H and δ^{18}O) of precipitation (4 sites) and a stream (1 site), and four contemporaneous stream sample sets of solute chemistry and isotopes, used to investigate watershed response to precipitation inputs in the 1780-ha Río Mameyes basin in the Luquillo Mountains of northeastern Puerto Rico. Extreme δ^2H and δ^{18}O values from low-pressure storm systems and the deuterium excess (*d*-excess) were useful tracers of watershed response in this tropical system. A hydrograph separation experiment performed in June 2011 yielded different but complementary information from stable isotope and solute chemistry data. The hydrograph separation results indicated that 36% of the storm rain that reached the soil surface left the watershed in a very short time as runoff. Weathering-derived solutes indicated near-stream groundwater was displaced into the stream at the beginning of the event, followed by significant dilution. The more biologically active solutes exhibited a net flushing behavior. The *d*-excess analysis suggested that streamflow typically has a recent rainfall component (~25%) with transit time less than the sampling resolution of 7 days, and a more well-mixed groundwater component (~75%). The contemporaneous stream sample sets showed an overall increase in dissolved solute concentrations with decreasing elevation that may be related to groundwater inputs, different geology, and slope position. A considerable amount of water from rain events runs off as quickflow and bypasses subsurface watershed flowpaths, and better understanding of shallow hillslope and deeper groundwater processes in the watershed will require sub-weekly data and detailed transit time modeling. A combined isotopic and solute chemistry approach can guide further studies to a more comprehensive model of the hydrology, and inform decisions for managing water supply with future changes in climate and land use.

Published by Elsevier Ltd.

1. Introduction

1.1. Forested mountain watersheds in the tropics

Forested mountain watersheds in the tropics are often characterized by higher annual rainfall amounts and frequency, greater energy inputs, and faster rates of human-induced change than watersheds in temperate latitudes (Bruijnzeel, 2004; Bruijnzeel et al., 2005; Ogden and Harmon, 2012; Wohl et al., 2012). In areas with frequent, high rainfall from seasonal monsoons or wet-season weather patterns, weathering is intense and bedrock evolves to clay soils. The presence of forests on steep mountain slopes provides soil structure for the storage and purification of water, controls erosion, enhances infiltration and recharge processes compared to cleared land (Bruijnzeel et al.,

* Corresponding author.
E-mail address: mascholl@usgs.gov (M.A. Scholl).

http://dx.doi.org/10.1016/j.apgeochem.2015.03.008
0883-2927/Published by Elsevier Ltd.

2005; Krishnaswamy et al., 2013), and may increase water yields during the dry season (Ogden et al., 2013). The high rainfall leads to ample runoff, and therefore water supply, under normal conditions, but the prospect of changing climate has led to uncertainty about the resilience of these systems under conditions of decreased rainfall or drought. These watersheds are essential to water supply for human populations and ecosystems, but factors that govern water supply, such as recharge rates and groundwater storage capacity, are often poorly quantified.

The Río Mameyes watershed is in the El Yunque National Forest (EYNF), contiguous with the Luquillo Experimental Forest (LEF) in eastern Puerto Rico. Research has been conducted in this tropical forest for decades by the U.S. Forest Service (USFS), the Luquillo Long Term Ecological Research (LTER), the U.S. Geological Survey (USGS) Water, Energy and Biogeochemical Budgets (WEBB), and the National Science Foundation (NSF) Luquillo Critical Zone Observatory (CZO) programs. The Mameyes watershed provides a high level of ecosystem services for Eastern Puerto Rico and the greater San Juan metropolitan area, which has a population >2.6 million (U.S. Census Bureau, www.census.gov). The Río Mameyes is designated as a wild and scenic river with minimum flow requirements, so aside from wells and stream withdrawals for National Forest operations, water withdrawals are at low elevations downstream of the forest boundary. In 2004, withdrawals accounted for 7 percent of annual stream runoff (Crook et al., 2007); since then there has been further development in the coastal areas, and groundwater well withdrawals were not included in the Crook et al. (2007) water budget. In addition to an abundant clean water supply, the watershed provides habitat for threatened species, biodiversity, recreation, and erosion control. Though global climate models have projected increased drying in the Caribbean (overview in Scholl and Murphy, 2014), Beck et al. (2013), Scholl and Murphy (2014) and Van Beusekom et al. (2015) have noted increases in rainfall amount, rain intensity, and minimum temperatures over the past two decades in eastern Puerto Rico and the Luquillo Mountains. This discrepancy between projections and observations of rainfall amount indicates that further research is needed to determine the effects of changes in temperature and rainfall patterns on watershed runoff response.

1.2. Stable isotope methods in tropical hydrology

Stable isotopes can be a useful tool to characterize and monitor hydrology in forested tropical watersheds (Bonell et al., 1998; Buttle and McDonnell, 2005; Klaus and McDonnell, 2013). Early studies that used isotope methods in high-rainfall watersheds are reviewed by Bonell et al. (1998) in their comparison of the Maimai, New Zealand (wet temperate) and Babinda, Queensland, Australia (wet tropical) studies. The tropical catchments were characterized by extremely rapid response of streamflow to rainfall, predominance of 'new' event water in the stream hydrographs, and a bypassing of groundwater storage during high intensity, high amount rain events. This flow pattern resulted from tropical clay soils with low permeability that caused water to flow laterally to the streams through high-permeability, near-surface flowpaths or saturation-excess overland flow during intense rain events (summarized in Elsenbeer, 2001). In contrast to many previous studies, storm flow did not mix with or displace previously stored water (Bonell et al., 1998). Similar flow mechanisms have also been observed in other tropical catchment studies (Elsenbeer et al., 1995; Schellekens et al., 2004; Goller et al., 2005; Bonell, 2005; Kurtz et al., 2011), and in a temperate forest on granitic bedrock (Burns et al., 2001).

Although the majority of runoff generation studies in tropical catchments have shown a predominance of lateral flowpaths in the watershed response to rainfall (Bonell, 2005), flow behavior depends on the vertical permeability structure in the hillslope subsurface. Notably, Muñoz-Villers and McDonnell (2012, 2013) used a series of isotope hydrograph separation experiments to investigate runoff generation processes in high-permeability volcanic substrate in Mexico during the transitional period between the dry season and the wet season, and compared results at pasture, secondary forest, and mature forest sites. Shallow lateral flowpaths were less important than vertical infiltration of recharge that displaced stored groundwater into the stream. They found that increasing percentages of pre-event water contributed to storm hydrographs in the first-order catchment over the course of the seasonal wetting-up cycle (Muñoz-Villers and McDonnell, 2012).

1.3. Previous work in the Luquillo Mountains

Extensive work has been done on the solute chemistry and hydrology of watersheds of the Luquillo Mountains (summarized in Murphy and Stallard, 2012a). At a regional scale, Scholl et al. (2009) and Scholl and Murphy (2014) characterized seasonal and climatic controls on the stable isotope composition of rainfall in eastern Puerto Rico, and utilized stable isotopes to determine sources of groundwater recharge and stream baseflow.

In and near the Río Mameyes basin, many of the studies linking chemistry to watershed response have focused on smaller watersheds or sub-catchments and yielded information on the sediment, solute and nutrient fluxes, hydrology, and geochemical cycling. McDowell and Asbury (1994) analyzed dissolved and particulate organic carbon, nutrients, major ions and sediment exports from 3 watersheds in the EYNF, the Icacos (326 ha), the Sonadora (262 ha) and the Toronja (16.2 ha). They suggested that the stream-water solutes under biotic control (NO_3, K, SO_4) were poorly correlated to changes in stream flow, while solutes related to geochemical processes and weathering (Na, Ca, Mg, HCO_3, Cl and SiO_2) had a strong inverse relationship with stream discharge, with dilution at high flows. Dissolved organic carbon (DOC) was hypothesized to be controlled by flow-path and soil structure. Schellekens et al. (2004) investigated stormflow generation processes using solute chemistry and discharge data in the 6.4-ha Bisley II sub-catchment of the Río Mameyes watershed. With soil water, precipitation, return flow and baseflow mixing model end members, they determined that the watershed response to rainfall was dominated by fast, shallow flowpaths. Questions remained about the relative importance of saturated overland flow versus macropore flow in the generation of runoff, as their roles in the rapid stormflow response could not be distinguished. As part of the study, a geophysical survey was done to measure resistivity in transects along and perpendicular to the streambed of the small stream. Results indicated that the saprolite-bedrock contact may be a prominent flowpath in the watershed (Schellekens et al., 2004).

Shanley et al. (2011) compiled long-term records of stream chemistry in the Río Icacos, a watershed in quartz diorite bedrock located on the other side of the ridge from the volcaniclastic Mameyes watershed. They observed that stream chemistry during rain events shifted toward the chemical composition of rainfall, becoming diluted by 90% or more from baseflow composition. The response of DOC indicated near-surface flowpaths contributed to quickflow during hydrograph peaks. Comparing Río Icacos to the 59 diverse watersheds evaluated for chemostatic behavior by Godsey et al. (2009), Shanley et al. (2011) found that for weathering solutes, Río Icacos was among the least chemostatic, i.e. most prone to dilution with increased flow. Kurtz et al. (2011) used $\delta^{18}O$ and Ge–Si tracers in the Río Icacos watershed and found three components contributing to the storm event hydrograph. The two predominant sources for streamflow were interpreted to be

Please cite this article in press as: Scholl, M.A., et al. Stable-isotope and solute-chemistry approaches to flow characterization in a forested tropical watershed, Luquillo Mountains, Puerto Rico. Appl. Geochem. (2015), http://dx.doi.org/10.1016/j.apgeochem.2015.03.008

groundwater and fast flowpath soil water (quickflow), with a smaller contribution of matrix soil water during the hydrograph recession.

The region is characterized by flashy stream flow hydrographs (Schellekens et al., 2004; Murphy and Stallard, 2012b). Shanley et al. (2011) using solute-chemistry methods and Scholl and Murphy (2014) using isotopic methods both noted that the flashy response of stream flow to rainfall that is characteristic of the Luquillo Mountain watersheds could be explained by saturation excess, because of the high frequency of rainfall and resulting high antecedent soil moisture, combined with low-permeability, high-clay content soils. Streamflow recession curve analysis also indicated relatively low storage (i.e. low porosity or volume of soils or saprolite) in the local watersheds (Rivera-Ramirez et al., 2002; Murphy and Stallard, 2012b).

1.4. Purpose and relevance

This study was conducted in the Mameyes basin (~3473 ha), a ridge to ocean watershed that is a good example of a mesoscale system that serves as an important water supply for coastal communities and for mountain forest ecosystems at higher elevation. Previous watershed studies in the area have been at a smaller scale (6.4–326 ha) and limited to higher elevations (>200 m). Uncertainties remain as to how the flow of water from rainfall to the stream channel is partitioned into overland/near-surface soil, shallow hillslope groundwater, riparian-zone groundwater, and deep groundwater pathways. It is important to understand this partitioning to be able to plan for possible changes in groundwater recharge and streamflow resulting from climate-change related shifts in rainfall patterns, as well as land-use changes near the coast.

In this paper, we describe 8-year data sets of precipitation and stream isotope composition at monthly to weekly resolution and four contemporaneous (synoptic) stream sample sets of solute chemistry and isotopes collected from ridge to the coastal plain in the Río Mameyes basin. Groundwater samples were also collected from three wells in the watershed. A hydrograph separation experiment performed in June 2011 yielded complementary information from stable isotope and solute chemistry data, and seasonal fluctuation in the deuterium excess (*d*-excess) parameter is used to assess the transit time between rain infiltration and its discharge as baseflow. The results from both the long-term sampling and the hydrograph separation experiment are combined to form an overall conceptual model of the rainfall–runoff dynamics in the watershed, and to compare to previous findings. The larger-scale approach taken here can guide further studies to a more comprehensive model of the hydrology and inform decisions for managing water supply with future changes in climate and land use.

2. Methods

2.1. Site description

The Mameyes watershed (Fig. 1a) faces north–northeast, and extends from the ocean to the ridgeline of the Luquillo Mountains at maximum elevation in Eastern Puerto Rico (0–1050 m). The upper watershed is primarily underlain by volcaniclastic rock, quartz diorite, and contact-metamorphosed volcaniclastic rock surrounding the quartz diorite intrusion (Fig. 1b). The lower watershed consists of volcaniclastic rocks, a small area of exposed mafic dikes, and alluvium in the stream valleys (Seiders, 1971). Soils at higher elevations in the Mameyes watershed are oxisols and inceptisols (Murphy et al., 2012), which are clay or clay loam soils that appear to behave hydrologically like Elsenbeer's (2001) "Acrisol" end-member in that they have decreasing saturated hydraulic conductivity with depth (Stallard and Murphy, 2012). The hydrograph separation data and the long-term stream isotope data set were collected at the U.S. Geological Survey (USGS) stream gage 50065500 Río Mameyes near Sabana within the EYNF, which we refer to in this paper as Río Mameyes at Puente Roto (MPR; Fig. 1). The site is at 84 m above sea level, with a 1780 ha drainage area above the gage. The watershed above MPR is entirely within EYNF, and is wet tropical montane forest that changes with increasing elevation from tabonuco through palo colorado and sierra palm forest, to cloud forest at the highest elevations. The watershed below MPR has mixed urban and low-density residential land use, pasture and moist tropical forest. Mean annual rainfall in the watershed is high, and varies with elevation from under 2000 mm y^{-1} at the coast, to 2690 mm y^{-1} at MPR (USGS, unpublished data), to 4200 mm y^{-1} at the top of the watershed (Murphy and Stallard, 2012b, their Fig. 4). Precipitation varies with season, with the wettest months being May–November, and the driest months December–April, but rainfall is relatively high year round in the mountains due to orographic effects (Heartsill-Scalley et al., 2007; Scholl and Murphy, 2014).

2.2. Rain, stream water and groundwater stable isotope monitoring

Cumulative monthly rain isotope samples were collected from four sites for 8 years (April 2005–June 2013; Scholl et al., 2009, 2014) and analyzed for δ^2H and $\delta^{18}O$. The Mameyes/Platanos site (MP, 5 m) was on the coastal plain, the Bisley site (BIS, 482 m) was on a tower above the forest canopy, and the Pico del Este site (PDE, 1011 m) was on the ridgeline that bounds the Mameyes watershed, 1–2 km to the east of the Mameyes watershed (Fig. 1a). We assume that PDE data represent isotopic and chemical compositions along the entire ridgeline within EYNF. The fourth long-term site was in the Icacos basin (ICA) at 694 m. The rain samples were collected using funnels on 20-liter HDPE carboys, with mineral oil added in a 1-cm thick layer over the water sample to prevent evaporative isotopic fractionation (Scholl and Murphy, 2014).

Cumulative weekly rain samples collected at PDE from February through July 2010 and from January 2011 to April 2013 were analyzed for stable isotopes. Samples were collected using a 17.6 cm diameter funnel that drained to a carboy. Rainfall was measured with a tipping bucket gage located on the same tower. Evaporation of the weekly samples was negligible, confirmed by comparing the weighted average weekly isotopic composition with isotopic composition of the monthly sample from the same site.

Stream water stable isotope samples were collected monthly from November 2007 to March 2010, and weekly from March 2010 to April 2013 at MPR. Grab samples were taken in 60 mL glass bottles with conical-insert caps. Groundwater samples were collected from three USFS water-supply wells at 461, 645 and 694 m elevation within the watershed, located approximately 1–2 km from the main channel of the Río Mameyes. The upper two wells are adjacent to the Río de la Mina, a large tributary of the Río Mameyes (Fig. 1b). Samples were collected from the pump spigot after pumping at least 3 well volumes, in June 2011 and May 2012, and analyzed for major ions, δ^2H and $\delta^{18}O$. Data are given in Appendix 1. Long-term mean solute chemistry data for rain at the Bisley lower tower, and for rain and cloud water from Pico del Este, were obtained from Gioda et al. (2013).

Samples of rainfall and stream water were analyzed for δ^2H and $\delta^{18}O$ at the USGS Reston Stable Isotope Laboratory, either by CRDS spectroscopy (precipitation) or by isotope-ratio mass spectrometry (streams and groundwater) using a hydrogen-

Please cite this article in press as: Scholl, M.A., et al. Stable-isotope and solute-chemistry approaches to flow characterization in a forested tropical watershed, Luquillo Mountains, Puerto Rico. Appl. Geochem. (2015), http://dx.doi.org/10.1016/j.apgeochem.2015.03.008

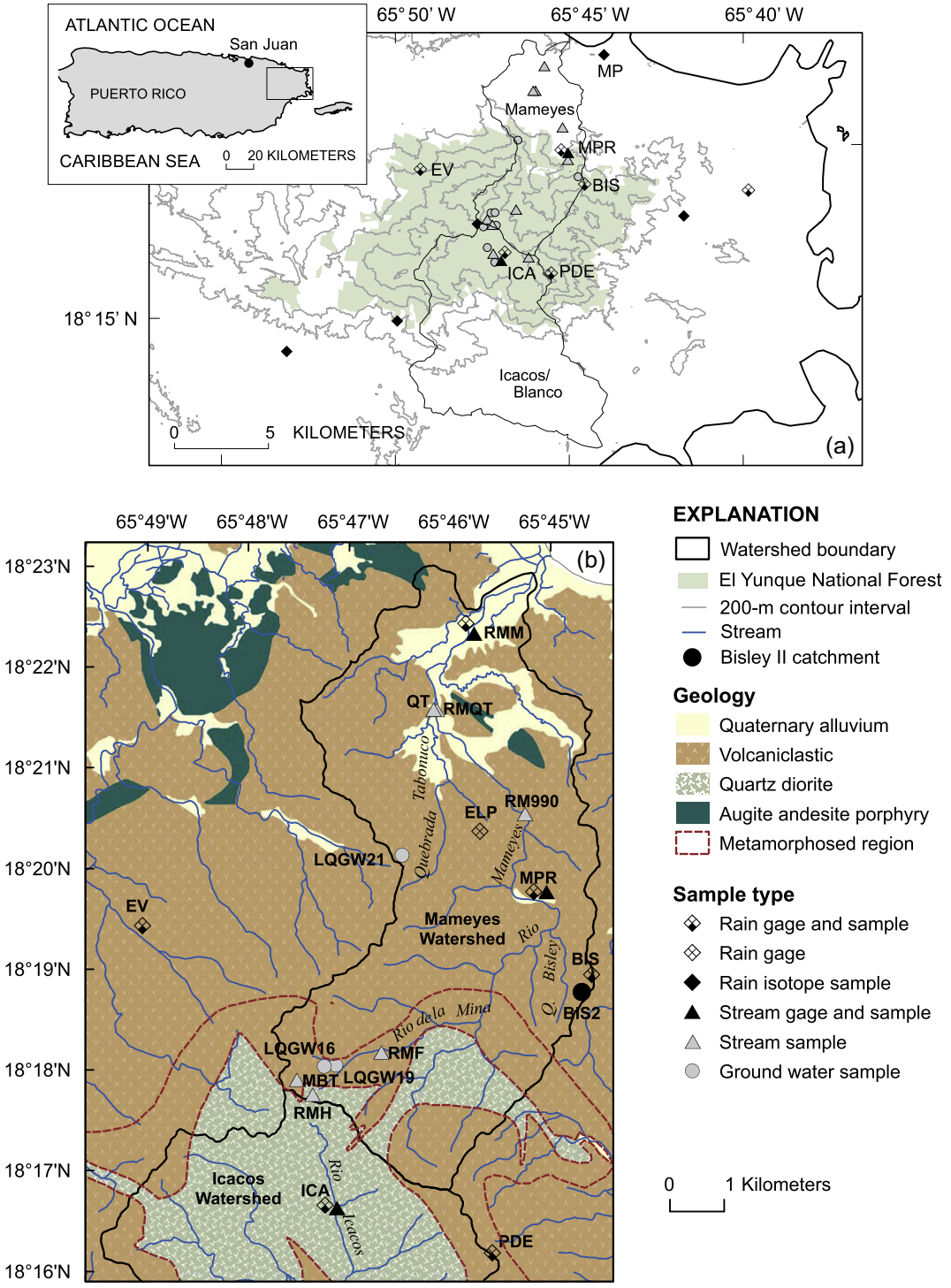

Fig. 1. (a) Map of eastern Puerto Rico, showing the Luquillo Mountains, the El Yunque National Forest, the Río Mameyes and Río Icacos/Río Blanco watersheds, and other sampling sites used in interpretation of results. Site name abbreviations: MP = Mameyes/Platanos, MPR = Río Mameyes at Puente Roto (USGS gage 50065500), BIS = Bisley tower, PDE = Pico del Este, ICA = Río Icacos (USGS gage 50075000), EV = USFS El Verde Research Station. (b) Map of the Mameyes watershed, showing geology, stream drainage networks, and sampling sites (adapted from Murphy et al., 2012 and Bawiec, 1998). The three-letter site name abbreviations that are not discussed in the text are listed in Appendix 1b.

equilibration technique for δ^2H and a CO_2 equilibration technique for δ^{18}O (Révész and Coplen, 2008a, 2008b). The 1-sigma analytical uncertainties of oxygen and hydrogen isotopic values are 0.1‰ and 1‰, respectively. Stable isotope data for rain, stream and groundwater samples are given in Appendix 1 or in Scholl et al. (2014).

2.3. Contemporaneous sampling

Five sets of contemporaneous (synoptic) stream samples were collected along the length of the Río Mameyes (Fig. 1b), from sea level to headwaters over a 2–3 day period during different seasons, in February 2006, November 2006, September 2007, June 2008,

and January 2010. The samples were taken under conditions that were at or near baseflow. Isotopic composition of the samples was used to determine recharge sources along the length of the stream, and major ion chemistry was used to infer relative contributions of groundwater with elevation in the watershed. Data are given in Appendix 1.

Samples for major ion chemistry analysis were filtered immediately through 25 mm diameter Whatman® GD/X filters which had a coarse glass-fiber prefilter and either a 0.45 μm polyethersulfone (PES) or glass fiber membrane. Cation samples were collected in acid-washed HDPE bottles and preserved with ultrapure HNO_3. Anions were collected in clean HDPE bottles. Separate samples for alkalinity analysis were collected in glass bottles for two of the sets, HDPE for others. All samples were refrigerated until analysis. Samples were analyzed at USGS research laboratories.

2.4. Hydrograph separation

A hydrograph separation was performed June 6–7, 2011 at the MPR site. Previous work in the area (Scholl et al., 2009) indicated that rainfall from low-pressure systems had a significantly depleted isotopic signature and thus this storm type would provide an accurate tracer of rainfall for hydrograph separation experiments. The source of the June 7, 2011 rain event was a persistent low-pressure system in the southwestern Caribbean Sea. Rain samples were taken at the site by sequentially filling 11-mL sample vials with a funnel throughout the period of rainfall. Six pre-event isotope samples were taken from the stream, and the stream was sampled for stable isotopes at approximately 20-min intervals for 6.5 h during the storm hydrograph, then once on each of the two subsequent days. Six samples for suspended sediment and solute chemistry were collected at approximately 20-min intervals during the peak storm hydrograph. Samples were analyzed for dissolved solutes at the University of New Hampshire Water Quality Analysis Laboratory. Storm rainfall was not collected for solute chemistry.

The isotope hydrograph separation utilized a two-component mixing model, with the tracers being δ^2H and $\delta^{18}O$ of event water (rainfall, EV) and pre-event water (groundwater/baseflow, GB). A single, intensity-weighted isotopic value was calculated for the entire rain event and utilized as the EV end member ($\delta^{18}O$, δ^2H of −128‰, −17‰; details in Section 3). The mean composition of the 3 groundwater wells, median long-term baseflow, and pre-event baseflow were the same within analytical error ($\delta^{18}O$, δ^2H were −2.63‰, −6.4‰ for groundwater and −2.53‰, −5.7‰ for median baseflow, respectively. Pre-event baseflow and GB end member was −2.52‰, −6.0‰). The following equation was used to determine the fraction of event rainfall (f_{EV}), which we define as quickflow, in each stream (S) sample:

$$f_{EV} = (\delta_S - \delta_{GB})/(\delta_{EV} - \delta_{GB}) \quad (1)$$

where δ_{EV} is the storm event rainfall end-member value of $\delta^{18}O$ or δ^2H, δ_{GB} is the pre-event water end-member value of $\delta^{18}O$ or δ^2H; and δ_S is the isotopic value of the stream sample for which the fraction of storm event water (quickflow) was determined. Most rain and stream samples were taken during the 4-h rain event, and the duration of the storm hydrograph was 54 h. Two isotope samples were taken from the stream on subsequent days, and the fraction of storm runoff was estimated by interpolation between those sample points using a log-linear relation.

2.5. Transit time estimate using deuterium excess

Deuterium excess (*d*-excess; Dansgaard, 1964) was calculated using the δ^2H and $\delta^{18}O$ values of the water samples:

$$d\text{-excess} = \delta^2H - 8 * \delta^{18}O \quad (2)$$

For the isotopic composition of a water sample plotted in $\delta^{18}O$-δ^2H space, the *d*-excess in units of per mil (‰), quantifies the vertical offset (along the δ^2H axis) of the sample from the original global meteoric water line (Craig, 1961):

$$\delta^2H = 8 * \delta^{18}O + 10 \quad (3)$$

The value of the *d*-excess is related to evaporative fractionation of isotopes and the temperature and humidity conditions during evaporation. The *d*-excess of rainfall can vary due to differences in ocean temperature and humidity in the water vapor source regions for precipitation (Merlivat and Jouzel, 1979; Lewis et al., 2013), local climate and land cover, and history of the air mass producing rain. Many studies have used *d*-excess to characterize recycled evapotranspiration vapor in the water cycle (e.g. Salati et al., 1979 for the Amazon region). Gat et al. (1994) used *d*-excess to determine the contribution of evaporation from the Great Lakes in the USA to the regional atmospheric water budget. Kabeya et al. (2007) utilized the *d*-excess parameter as a tracer of residence time in a study of a small headwater catchment in Japan. The parameter has not been used extensively as a tracer in watershed hydrology studies, but can be useful to partition water into different sources for hydrograph separations (Lyon et al., 2009) and to investigate water use by plants (Dawson and Simonin, 2011). The *d*-excess of rainfall in eastern Puerto Rico varies both by season (rainfall vapor source) and by elevation in the watershed, and *d*-excess is a better signal for seasonality than the isotope ratios (explained in detail in the results, Section 3.3). Adapting the approach used by Kabeya et al. (2007), seasonal fluctuation of *d*-excess in weekly rainfall samples from PDE and in stream samples from MPR was used to estimate a mean transit time between the occurrence of rainfall and its arrival in the stream.

Normalized *d*-excess values (‰) for rain and stream time series were calculated as sample *d*-excess minus the mean *d*-excess value of the weekly rain (input) and baseflow (output) series. A sine function with frequency period of 365.25 days was fit to each series:

$$dx_{norm}(t) = A\sin(\omega t + \varphi) \quad (4)$$

where $dx_{norm}(t)$ is the 'departure from normal' *d*-excess value (‰), t is elapsed time since the beginning of sampling (days), A is the amplitude of the dx_{norm} function, ω is the angular frequency and φ is the phase shift. To obtain the best fit to the data, the amplitude and phase shift parameters were adjusted to minimize the square root of the mean squared error (RMSE) between observations and model. The estimate of mean transit time was the difference in phase (lag) between the input (rain) and output (stream) *d*-excess functions. This simple lag time estimate involves no assumptions about subsurface flow mechanisms, and is for the upper, forested 1780-ha area of the watershed, between the rainfall input at 1050 m and the stream baseflow output at 84 m.

3. Results

3.1. Groundwater and baseflow chemistry comparison

Solute concentrations in stream baseflow generally increased with decreasing elevation in the watershed. Fig. 2 shows concentration of individual constituents Ca, HCO_3, SiO_2, NO_3, Na, Cl, K, and SO_4, as a function of site elevation for the contemporaneous stream sample sets, the 3 groundwater wells in the upper Mameyes watershed, and mean rainfall concentrations from 1988 to 2007 at BIS (Gioda et al., 2013). The lowest sites (from elevation 5–12 m) drain areas that have a substantial amount of Quaternary alluvium, including the Quebrada Tabonuco, which

Please cite this article in press as: Scholl, M.A., et al. Stable-isotope and solute-chemistry approaches to flow characterization in a forested tropical watershed, Luquillo Mountains, Puerto Rico. Appl. Geochem. (2015), http://dx.doi.org/10.1016/j.apgeochem.2015.03.008

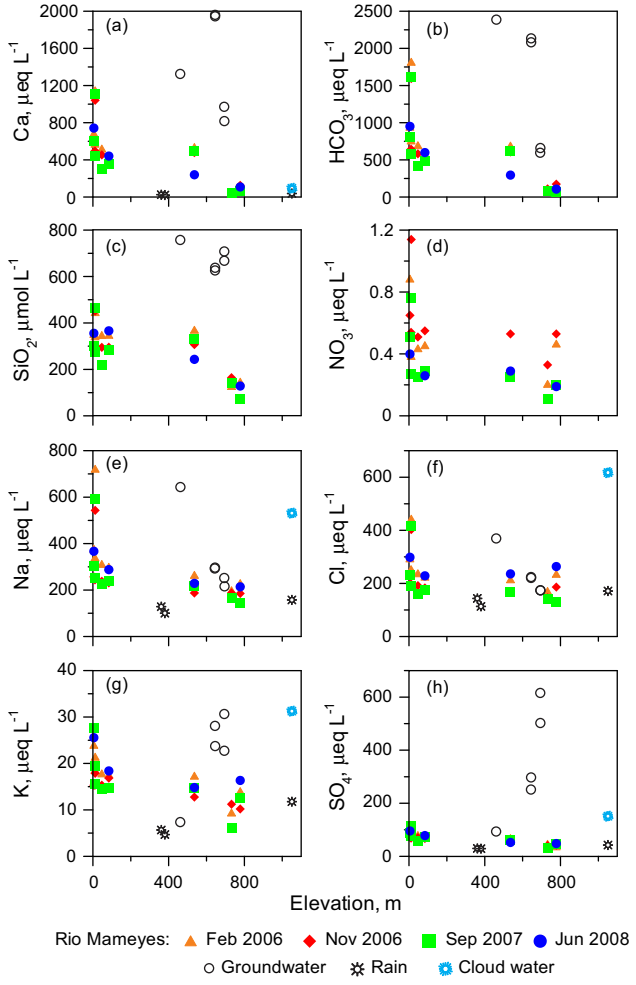

Fig. 2. Stream, groundwater and precipitation solute chemistry at elevations from 5 to 1050 m in the Río Mameyes watershed. Precipitation includes both rain and cloud water at 1051 m. All concentrations are in µeq l^{-1} except for SiO_2, which is in µmol l^{-1}. Chemical composition of precipitation is from Table 1 in Gioda et al. (2013) (did not include HCO_3 or SiO_2), and NO_3 was not analyzed for groundwater. Mg patterns (not shown) were similar to Ca; data available in Appendix 1.

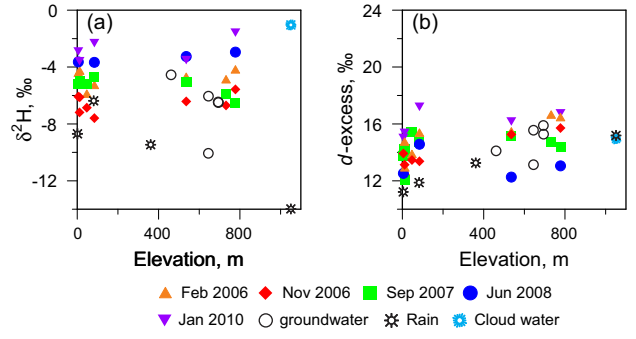

Fig. 3. (a) Stream, precipitation (rain and cloud water), and groundwater δ^2H versus elevation in the Mameyes watershed. Precipitation δ^2H values are volume-weighted averages (VWA) from Scholl et al. (2014); the two samples at 1050 m elevation are VWA rainfall (−14‰) and mean cloud water (−1‰). (b) Deuterium excess versus elevation in the watershed for the same samples, plotted on the same scale as Fig. 3a.

has the highest measured solute concentrations (Fig. 1b; Appendix 1a). Much of this stream's drainage area is outside the forest boundaries and has mixed residential, moist forest and pasture land. Lowest solute concentrations were observed at the two highest elevation sampling sites (732 m and 778 m). These perennial headwater tributaries drain igneous or contact-metamorphosed terrane. Sites in between these elevation end-members are located on volcaniclastic or metamorphosed volcaniclastic rock (Fig. 1b).

Dissolved Si, Ca, and HCO_3, which are derived primarily from bedrock weathering processes (Shanley et al., 2011; Stallard and Murphy, 2012, 2014), showed similar concentrations in stream samples from 5 to 536 m elevation in the Río Mameyes and its major tributary Río de la Mina, then decreased in the two highest elevation (732 and 778 m) headwater samples (Fig. 2a–c). Ca and HCO_3 concentration in stream samples varied more than SiO_2, partly because the high concentrations in the Quebrada Tabonuco tributary affect the Río Mameyes downstream of their confluence. The higher concentrations at low elevation may also reflect differing geology (Fig. 1b), flow through alluvium, or longer groundwater flowpaths and therefore longer contact time with saprolite or bedrock. Dissolved Cl, which originates from seasalt, and SO_4 and Na, which have both seasalt and bedrock sources (McDowell and Asbury, 1994; Shanley et al., 2011; Stallard and Murphy, 2014), had relatively small changes in concentration with elevation in the watershed, and Cl concentrations increased less than other solutes as elevation decreased (Fig. 2e, f and h).

Groundwater usually had higher solute concentrations than stream baseflow, with the exception of Na and Cl, for which the two higher-elevation wells and stream baseflow had similar concentrations (Fig. 2e and f). The lowest elevation well (LQGW21), which is located in volcaniclastic bedrock (Fig. 1b), had the highest concentrations of all solutes except K and SO_4. Concentrations of K and SO_4 in that well were closest to precipitation and stream samples (Fig. 2g and h), while the two higher-elevation wells, in metamorphosed rock, had significantly higher concentrations of SO_4. Concentration of SiO_2 was similar for all three wells.

Mean concentrations of Ca, Na, K, Cl, SO_4 and HCO_3 in rainfall, as expected, were lower than in streamflow or groundwater. Because of its smaller droplet size, cloud water has higher concentrations of solutes than rainfall, and concentrations of Na, Cl and K in cloud water were higher than in stream water, likely due to the significant marine aerosol source (Gioda et al., 2013).

While rainwater stable isotope values decrease with increasing elevation in the study area (Scholl et al., 2009), as is typical in isotope hydrology (Siegenthaler and Oeschger, 1980), the δ^2H composition of streamflow in the Mameyes watershed varied more with sampling date (season) than with elevation (Fig. 3a). Some stream sample sets even showed an increase in δ^2H value with increasing elevation (Fig. 3a). Because trade-wind rainfall and cloud water are isotopically enriched (higher δ value) relative to other types of rainfall, and this isotopically-enriched rainfall increases in amount with increasing elevation in the study area, the plot of elevation versus isotope value of stream water can have a zero or positive slope (Scholl et al., 2002; Scholl and Murphy, 2014). The *d*-excess of stream baseflow also varied with season more than with elevation. An increasing trend in *d*-excess from the lowest- to the highest-elevation sites is observed in the precipitation, but is only evident in the February and November 2006 stream sample sets (Fig. 3b).

3.2. Hydrograph separation results for the June 7, 2011 event

3.2.1. Stable isotopes

Results from the hydrograph separation at site MPR on June 7, 2011 are shown in Fig. 4. The moisture source for the rain event was a persistent low-pressure system in the southwestern Caribbean Sea; it produced rainfall that resulted in an exceptionally large difference (about 122‰ in δ^2H) between the storm rain and pre-event baseflow isotopic composition. Rainfall amount

Table 1
Rainfall timing, duration and amounts for June 7, 2011 at measurement sites in the study area (see Fig. 1 for site locations).

Rain gage	Elevation (m)	Gage resolution	Event time	Rainfall amount (mm)	Event duration (h)	Mean intensity (mm h^{-1})
MPR (rain collection site)	84	–	9:38–13:36	–	4.0	3.7*
El Portal (ELP)	184	5–15 min	9:30–14:15	33	4.8	6.9
Bisley Lower Tower (BIS)	352	hourly	9:00–19:00	52	10	5.2
Icacos (ICA)	645	5–15 min	9:20–18:20	95	9.0	10.6

* Estimated from time to fill sample vials.

and duration varied with elevation in the watershed (Table 1). The rain event duration at the MPR site was 4 h (9:38–13:36), and most stream samples for stable isotope analysis were taken during that period. Low-level atmospheric flow over the area was from the south and southeast, so the rain event had longer duration and larger amounts at the higher altitude and south-facing ICA site. This site is about 1 km from the ridgeline between the Icacos and Mameyes watersheds, so we used it as a proxy for the higher elevations in the Mameyes watershed. The event had a mean intensity of 3.7 mm h^{-1} at the MPR sampling site and 10.6 mm h^{-1} at the ICA site. A rain event $\geqslant$30 mm has a relative frequency of 7.7% for rain events >1 mm at MPR, and a $\geqslant$90 mm event has a relative frequency of 2% for events >1 mm at ICA (M.A. Scholl, unpublished data, 1992–2011). The total rainfall from BIS was used in the calculations to represent the event for the watershed, but the data are hourly, so rainfall from Icacos (645 m) and El Portal (184 m) stations (5–15 min resolution), are shown in Fig. 4c to illustrate the distribution of rainfall at high and low elevations over the event.

Isotopic values of rainfall were lowest during the high-intensity period at the beginning of the event, and ranged from −154‰ to −109‰ in δ^2H and −20.4‰ to −14.7‰ in δ^{18}O over the course of the event (Fig. 4b). Rainfall composition probably also varied with elevation, and the rain lasted longer at higher elevations, so that over the entire watershed area, event water isotopic composition would become homogenized with different travel times to the stream sampling point. Because we did not measure spatial and temporal variation of isotopic composition for the entire watershed, the single, intensity-weighted mean values of δ^2H = −128‰, and δ^{18}O = −17‰ were used for calculation of the proportion of quickflow in the stream hydrograph.

The June 7 rain event caused an increase in stream runoff (discharge) from 0.58 mm h^{-1} (2.9 m^3 s^{-1}) to 7.1 mm h^{-1} (35 m^3 s^{-1}) (Fig. 4d). Three smaller rain events prior to the hydrograph separation experiment provided antecedent moisture; rain events on June 2, 4 and 5 led to peak runoff values of 1.5, 4.7 and 1.3 mm h^{-1} (7.3, 23.1 and 6.6 m^3 s^{-1}), respectively, at MPR and the stream returned to baseflow very quickly after each event. This pattern is not unusual; rain in the Luquillo Mountains (primarily brief, low-intensity events) occurs on average every 8 h (Scholl and Murphy, 2014). Despite the high antecedent moisture in the watershed, the baseflow δ^2H, δ^{18}O composition measured at 9:20 on June 6 before the experiment was −6‰, −2.5‰, respectively, the same as the long-term median stream water isotopic composition at the MPR site. On June 7, stream runoff increased slightly in response to a period of rain around 3:00 (Fig. 4c), which also affected isotopic composition of stream water (Fig. 4b), then the bulk of the rainfall began at 9:30.

The lowest measured isotopic value of rainfall occurred at the beginning of the storm, allowing estimation of the transport time of storm rainwater to the stream. The lag time between the minimum rain isotopic composition and the minimum stream isotopic composition was 1.3 h, with a sampling time resolution for the stream of ~0.3 h. The average of results from δ^2H and δ^{18}O in the mixing model (Eq. (1)) showed that total event water (quickflow) draining the watershed on June 7 from 9:38 to 16:00 was 9.4 mm and total watershed runoff was 21.1 mm (Fig. 4d). Quickflow comprised 45% of total flow during the rain event. The isotope mixing model calculations indicated a quickflow fraction of 0.19 in the first sample. Some of this may have been saturation-excess overland flow, but we cannot rule out the presence of some event water in the stream channel because the rain began earlier at higher elevation in the watershed (Fig. 4c). Over the entire event hydrograph (54.5 h), rainfall was 52 mm, and 9.4 mm was conveyed quickly to the stream as runoff (the additional 10 mm of rainfall around 13:30 had little effect on the stream isotopic composition or the calculations, Fig. 4b). This 18% storm runoff estimate assumes no loss of rainfall prior to infiltration; however, there is as much as 50% canopy interception loss in this forest (Schellekens et al., 1999). Using this 50% interception assumption as Schellekens et al. (2004) did in their study, we estimate that 26 mm of storm rain reached the hillslope, of which 9.4 mm, or 36%, left the watershed as runoff.

3.2.2. Dissolved solutes

Two different types of response were observed in the stream solute concentrations during the rain event (Figs. 4a and 5). Fig. 4a shows the two types of solute behavior and sample timing in relation to the hydrograph, while Fig. 5 shows concentration of all the solutes as a fraction of the concentration of the first sample (taken ~15 min after the rain began, before the hydrograph rise). The behavior of Ca was similar to that of Mg, Na, SO_4 and Cl; all had higher concentrations in the second sample, followed by a decrease in concentration (dilution) that roughly coincided with the peak of the hydrograph (sample resolution was ~20 min). Concentrations showed increasing dilution for the next 70 min as the hydrograph receded, then concentrations began returning toward their original values in the last two samples. Potassium concentrations followed a similar pattern to the solutes discussed previously, but all sample concentrations were higher than the initial concentration. In contrast, concentrations of NH_4 and NO_3 in the stream initially decreased during the peak of the hydrograph, followed by an increase to more than double their initial concentrations; NH_4 then decreased to near its initial value in the last sample, while NO_3 increased.

3.3. Deuterium excess as a tracer

Weekly values of δ^2H in rain and stream samples from January 2011 to April 2013 are shown in Fig. 6a, at different scales so that the time series can be compared. The plot illustrates an overall correspondence between the precipitation and stream isotopic composition, but there are periods during which the two samples do not correspond as well. The rain sample is cumulative for the week, while the stream sample is instantaneous, so a sharp change in isotopic value in the rain record can represent storm water that passed through the stream system either before or after the stream sample was taken. The isotopic composition of the stream depends on rainfall amount and intensity as well as storm timing, and may respond less during periods when brief, low-intensity rain events predominate and less quickflow reaches the streams.

Please cite this article in press as: Scholl, M.A., et al. Stable-isotope and solute-chemistry approaches to flow characterization in a forested tropical watershed, Luquillo Mountains, Puerto Rico. Appl. Geochem. (2015), http://dx.doi.org/10.1016/j.apgeochem.2015.03.008

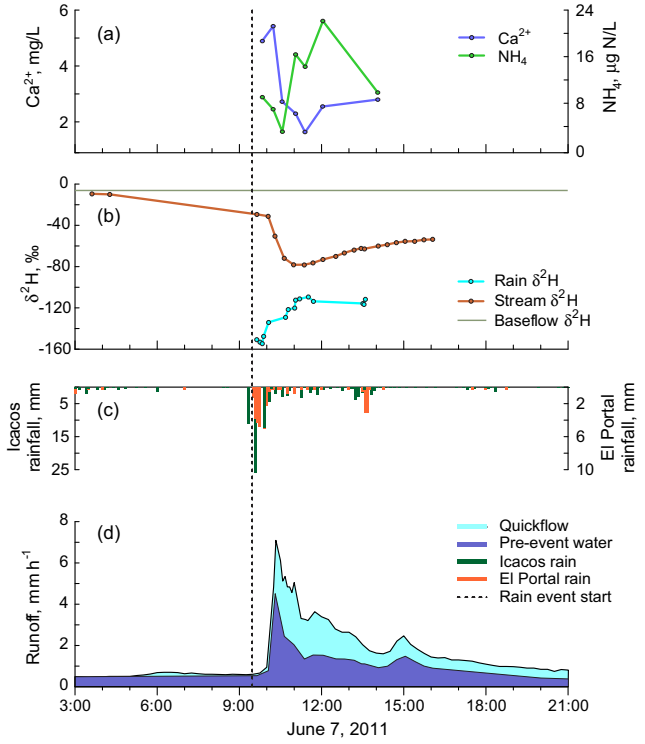

Fig. 4. Results of the isotope hydrograph separation experiment, showing (a) Ca and NH_4 concentrations in the Rio Mameyes at MPR, illustrating contrasting behavior of solutes, (b) δ^2H values of rainfall and stream water at MPR, (c) rainfall at the Icacos and El Portal stations, and (d) total runoff partitioned into pre-event water and quickflow, determined with Eq. (1). The vertical dashed line at 9:30 indicates the time rainfall began at the nearby El Portal gage; the first sample was collected at MPR at 9:38. The plot shows data for June 7 only; additional stream isotope samples were taken June 8 at 13:25 and June 9 at 16:05 and were used in the calculation of total storm runoff described in the text.

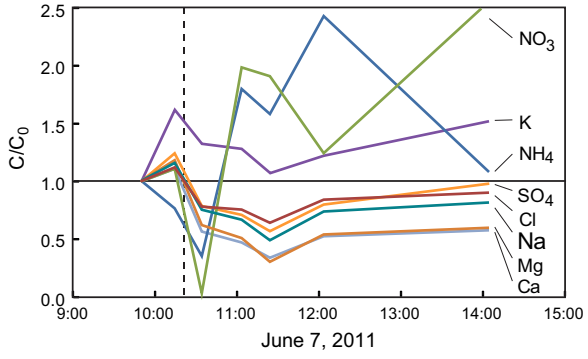

Fig. 5. Normalized concentration (C/C_0) of solutes measured in the Río Mameyes (MPR site) during the June 7, 2011 hydrograph separation experiment. The dashed vertical line shows the time of the peak of the hydrograph. The horizontal line indicates the initial normalized concentration (1.0).

Deuterium excess and δ^2H of rainfall over eight years for the PDE (1050 m) and MP (5 m) monthly-sample rain collector sites are plotted in Fig. 6b (the other sites have a similar pattern, as does the $\delta^{18}O$). The plot shows that monthly patterns of rain isotopic composition are similar throughout the Mameyes watershed; and that δ^2H is higher, while *d*-excess is lower, on the coastal plain (MP) than at the top of the mountains (PDE). Both the δ^2H and *d*-excess show seasonal variation, but the δ^2H record shows higher variability, especially between successive summer-fall wet

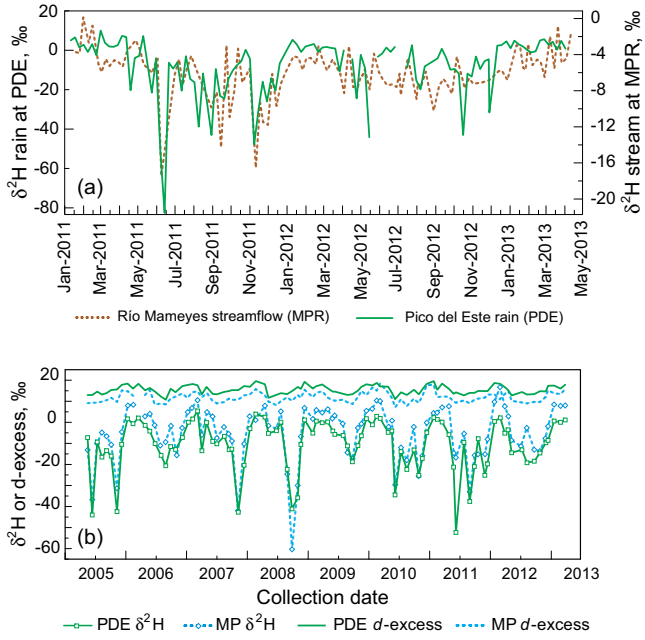

Fig. 6. (a) Weekly stream δ^2H from the Río Mameyes (MPR) and rain δ^2H from Pico del Este (PDE) from January 2011 through April 2013. Note the different scales for stream and rain time series. (b) Monthly rain isotope time series from 2005 to 2013 showing δ^2H and *d*-excess values at the Pico del Este (PDE, 1050 m) and Mameyes-Platanos (MP, 5 m) collection sites in the study area. The longer tick marks on the *x*-axis represent January 1 of each year.

seasons, than the *d*-excess. Rain from tropical storms, hurricanes, and other cyclonic low-pressure systems has an extremely depleted isotopic signature compared to other weather systems that bring rainfall to Puerto Rico (Scholl et al., 2009) and when these storms occur they dominate the composition of the weekly or monthly sample. Fig. 6b illustrates that *d*-excess can be a better signal for seasonality than the isotope ratios. The *d*-excess of rain that has extreme isotopic depletion is unremarkable, and similar to other summer precipitation, so the seasonal cycle of *d*-excess of rainfall is more uniform on a year-to-year basis than the isotopic ratios.

Like ^2H and ^{18}O, the *d*-excess of rainfall varies both by season (rainfall source) and by elevation in the watershed (Fig. 7). The highest *d*-excess in rainfall is observed December–March (Fig. 7), when precipitation is predominantly from the trade-wind orographic source. This precipitation is formed from water vapor below the atmospheric boundary layer, from approximately sea level to 2300 m (Scholl et al., 2009; Scholl and Murphy, 2014) and it likely includes local re-evaporated canopy interception and transpiration vapor (Simonin et al., 2013). The lowest *d*-excess values are observed June–August (Fig. 7), corresponding with rain from tropical waves and low pressure systems, condensed from water vapor from as high as 13 km in the atmosphere. The mean stream *d*-excess value of 14.6‰ is between the mean annual values from the higher elevation sites: PDE (1050 m), BIS (482 m) and ICA (616 m).

A mean transit time estimate was made using the weekly records of rain and stream stable isotopes. For each dataset, the *d*-excess was calculated and normalized as the deviation from the mean *d*-excess, and the seasonal cycle was fit with a sine function (Fig. 8a). The best fit of the sine function to the data was obtained by minimizing the root mean squared error (RMSE). Because the stream *d*-excess varied less than the rain, the fit to the stream data was better than to the rain data (RMSE 0.87 and 1.85 respectively). To evaluate whether *d*-excess was a conservative tracer for this system, we calculated the expected stream

d-excess given the average proportions of 59% trade-wind orographic and 41% convective precipitation as determined in Scholl and Murphy (2014). The mean stream *d*-excess of 14.6‰ agreed with the expected value of 14.1‰, indicating that the water discharging to the stream does not include appreciable amounts of evaporated soil water (which would have a *d*-excess value <10‰).

The amplitude of streamwater *d*-excess seasonal variation (0.7‰) was smaller than that of the rain (2.5‰). The phase lag between rain and stream *d*-excess cycles was 2.2 days, but because rain and stream were not always sampled on the same day, this has to be interpreted as ⩽7 days, the weekly sampling resolution (Fig. 8a). The lag time can also be estimated using rain events with a strongly depleted isotopic signature, but only for rain events when the rain sample was collected before the stream sample (cf. Fig. 6a). For the few events in the data record where this occurred, the lag time between the rain and change in stream isotopic composition was 1–2 days, in overall agreement with the results from the seasonal *d*-excess evaluation shown in Fig. 8a. Since there was no appreciable lag between the rain (input) and stream (output) isotopic series, we did not pursue the piston flow/exponential flow conceptual models for hillslope flowpaths, as outlined in Kabeya et al. (2007).

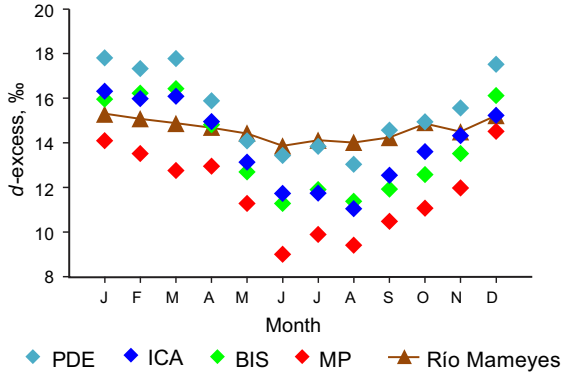

Fig. 7. Mean monthly *d*-excess of rainfall and streamflow, derived from monthly data from 2005 to 2013 at the 4 long-term rain sites and monthly and weekly data from 2007 to 2013 from the Río Mameyes at MPR. The standard deviation ranged from 0.7‰ to 2.2‰ on the monthly average values.

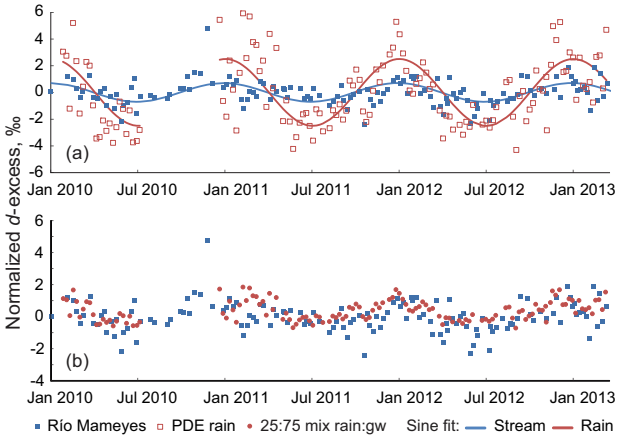

Fig. 8. (a) Normalized *d*-excess (deviation from mean) calculated for weekly rain samples at PDE and weekly stream samples at MPR for the period January 2010 to October 2012, with the seasonal sine function fit to each data set. Weekly rain samples were not collected August through December 2010. (b) Time series of normalized *d*-excess for stream water, and for a mixture of 25% rain, 75% groundwater using *d*-excess values for each rain sample and mean groundwater.

The output (stream) *d*-excess signal is smaller in amplitude (damped) compared to the input (rain) signal (Figs. 7 and 8), and this is observed in the δ^2H data as well (Fig. 6a). The simplest conceptual model that explains the observed results is that baseflow (at the scale of the watershed measured at the MPR site) is comprised of one component with short residence time (recent rainfall, transit time ⩽7 days) and another component (well-mixed groundwater) with relatively uniform isotopic composition. Using a two-component mixing calculation with the *d*-excess values of each rain sample and mean groundwater, the best match to the amplitude of the stream signal is 25% recent rain, 75% groundwater (Fig. 8b). There are periods (winter 2011, summer 2012) where the highest *d*-excess values in rain were not observed in the stream, suggesting that the patterns of rainfall amount and frequency affect temporal variation in proportions of quickflow and baseflow in the stream.

4. Discussion and conclusions

The overall increase in dissolved solute concentrations with decreasing elevation that was observed in the Río Mameyes is consistent with increasing flowpath lengths for groundwater entering the stream from the ridgeline to the coast, and also with different geology at lower elevations in the basin (Fig. 1). The Río Mameyes and its tributaries drain several types of bedrock, in addition to alluvial sediments, as it runs to the ocean (Fig. 1b). In the quartz diorite Icacos watershed, Bhatt and McDowell (2007) found that the headwater samples taken on steep slopes had higher concentrations of solutes, including weathering products Si and HCO_3, than lower elevation and mainstem stream samples. They postulated that landslides exposed fresh reactive mineral weathering surfaces in the headwaters, while the mainstem of the Rio Icacos was relatively dilute. In contrast, the high-elevation Mameyes samples in this study had the lowest solute concentrations, while the highest solute concentrations were observed in groundwater; and solute concentrations increased with decreasing elevation.

The Río Mameyes stream profile displays a traditionally concave shape – indicating that the stream is graded to current base-level (sea level). However, along the Río Mameyes, the longitudinal profiles show small scale steepening and pronounced convexity at the boundary between contact-metamorphosed rock in the upper basin and the volcaniclastic rock downstream (Pike et al., 2010). In contrast, the stream profile of the Rio Icacos is convex with a zone of steepened topography and river gradient (knickzone). The knickzone separates a subdued upstream portion of the landscape (>600 m asl) characterized by a thick saprolite, from which non-recalcitrant minerals have been weathered (White et al., 1998; Murphy et al., 1998), from a downstream landscape where incompletely weathered minerals remain in the saprolite and soils. Mineral assemblages below and above the Rio Icacos knickzone may be a major control on the pattern of increases of weathering-flux solutes below the elevation of 600 m (Brocard et al., this issue); similar differences in the degree of weathering may partly explain changes in stream chemistry with elevation in the Mameyes watershed as well.

Our results indicated that SiO_2 is the best overall tracer for deeper groundwater input in the Mameyes watershed; the 3 groundwater well samples had similar concentrations, and dissolved Si is derived from bedrock and soils whereas many of the other solutes originate from both seasalt and mineral weathering. Concentrations of Si indicate that deep groundwater input increases as the stream elevation decreases (Fig. 2a). The largest difference in concentration between groundwater and stream baseflow was for SO_4. Sulfide-containing minerals present in the metamorphosed volcaniclastic bedrock (Bawiec, 1998) may have

Please cite this article in press as: Scholl, M.A., et al. Stable-isotope and solute-chemistry approaches to flow characterization in a forested tropical watershed, Luquillo Mountains, Puerto Rico. Appl. Geochem. (2015), http://dx.doi.org/10.1016/j.apgeochem.2015.03.008

contributed to SO_4 concentrations in the groundwater in the upper watershed. At lower elevation, sulfur isotopes indicated that bedrock was a significant source of sulfate to streamflow in the Bisley watershed (BIS, Fig. 1) within the Mameyes basin (Yi-Balan et al., 2014), and Buss et al. (2013) observed pyrite and other sulfide minerals in a drill core in the Bisley watershed.

Hydrograph separation results indicate that the Mameyes watershed has a similar response to storm rainfall as seen in other tropical studies with low permeability below the top layer of soil, lateral flow, and fast runoff of a significant portion of storm rainfall (Bonell et al., 1998; Elsenbeer, 2001; Bonell, 2005). The combination of isotope and solute chemistry techniques showed different aspects of the watershed response. The isotopes indicated immediate flow of event water into the stream in response to the storm event (0.19 quickflow fraction in the first sample), which may have been due to saturation-excess overland flow and/or event water in the stream channel from higher elevations (Fig. 4). This was followed by a relatively high fraction of storm-event quickflow during the peak portion of the hydrograph (0.48 within 4 h, with a maximum of 0.60 at peak flow). The large difference between rain and baseflow isotope values led to a very good estimate of quickflow and pre-event water in the hydrograph separation. Based on patterns in the weathering-derived solutes (Fig. 5), a small amount of near-stream groundwater was displaced into the stream at the beginning of the event, followed by significant dilution, then concentrations reflected a return to baseflow chemistry. The more biologically active solutes (NO_3, NH_4 and K) exhibited a net flushing behavior. NO_3 and NH_4 concentration were low, but showed a coherent pattern of dilution during the peak of the hydrograph, after which the concentrations remained above their pre-storm levels. K concentrations also showed net flushing, but after an initial increase they tracked base cation behavior, reflecting dual sources in mineral weathering and biological cycling. The results suggested that the watershed response to storm event rain includes near-stream pre-event groundwater, and shallow soil-overland flow components. These details of the flow pattern would not have been observed if only one tracer, either isotopes or solutes, had been used.

The fraction of storm quickflow runoff in the Mameyes watershed compared to the smaller Bisley sub-catchment suggests that the runoff response is broadly similar at both scales. Schellekens et al. (2004) measured quickflow in the Bisley II watershed for 31 storm events using a simple straight-line hydrograph separation method. Rainfall in the events ranged from 3.2 to 227 mm. They found that on average 9% (max 28%) of the precipitation during storm events left the catchment as quickflow, which they translated to 18% (max 56%) considering interception losses. This compares with 36% in our experiment. Their 55 mm event had a quickflow/precipitation (QF/P) ratio of 0.23. Our QF/P ratio at MPR was smaller (0.17) but the watershed area is much larger than that of the Bisley II (1780 versus 6.4 ha). For both of these studies, the assumption of 50% canopy interception loss was used to adjust the quickflow runoff fraction of the storm hydrographs. Although Schellekens et al. (1999) found that interception losses were ~50% regardless of storm size for Bisley, further studies on variation in canopy interception with rainfall intensity elsewhere in the Mameyes watershed would help to quantify this source of uncertainty.

The hydrograph separation results indicated that 36% of the storm rain that reached the soil surface left the watershed in a very short time period as runoff. The partitioning of the other 64% remains a question for further research, since the isotopic composition of the stream was back to near pre-event values in 2.5 days, shortly after discharge returned to baseflow. In the Babinda tropical catchment, which had a similar high percentage of event water in the storm hydrographs, stream isotope values reflected the presence of storm event water after the discharge returned to baseflow (Bonell et al., 1998). Similar delayed transport of event water was observed in isotope hydrograph separations for several Panama catchments with different land cover (Litt et al., this issue). In contrast, no delayed discharge of event water was observed for the June 7, 2011 storm event in the Mameyes watershed. The extremely depleted values from this storm would have been detected if the storm water continued to contribute to the stream from a hillslope shallow groundwater reservoir over time. June is near the beginning of the wet season, and flow dynamics in the watershed may change as the season proceeds (Muñoz-Villers and McDonnell, 2012); it would be informative to perform similar repeated studies over seasonal transitions at this site.

Though there was not an appreciable lag time detected between rain inputs and runoff for this watershed, our results demonstrated that *d*-excess can be a useful tracer in addition to δ^2H and $\delta^{18}O$, and may work well in other tropical watershed studies. The analysis suggested that the flow system has a recent rainfall component with $\leqslant$7-day residence time (~25%) and a well-mixed groundwater component (~75%). We assume that the rainfall that infiltrates is partitioned into hillslope groundwater storage, deeper groundwater storage, and soil water that supplies evapotranspiration processes, but the isotope values in this study do not distinguish stream baseflow from groundwater in wells, so it is difficult to partition streamflow further than quickflow and groundwater components. Longer groundwater flowpaths, with more time in contact with subsurface minerals, are evidenced by the higher concentration of dissolved solutes in well samples compared to stream baseflow. Additional analysis of dissolved solutes in groundwater and soil may be helpful in partitioning hillslope and deeper groundwater inputs to the stream. Deep groundwater may contribute to the stream near sea level, and possibly also to submarine discharge, so groundwater samples from the lower elevations in the Mameyes watershed would be helpful in determining the eventual distribution of rain water from the larger storms. Further work to model transit-time distributions (e.g. Weiler et al., 2003; Muñoz-Villers and McDonnell, 2012; Timbe et al., 2014; Harman, 2015) will help to refine the initial approximation presented here.

By considering a larger scale than most previous studies in high-rainfall northeastern Puerto Rico, we were able to optimize the use of the long-term rain stable isotope database for the area, and the results are relevant to the typical scale of water extraction for municipal water supply. Based on an extreme isotopic depletion of the input rainfall, our hydrograph separation was quite robust. Accordingly, our finding of 36% event water in the hydrograph separation demonstrated that in this moderate-sized storm, a considerable amount of water ran off as quickflow and bypassed deeper watershed flowpaths. This finding corresponds well with the brief lag time (less than or equal to the sampling resolution of 7 days) between rainfall and runoff isotopic composition that was shown by the *d*-excess analysis at the 1780-ha scale of the watershed over 3.3 years of weekly data. These initial results for the watershed indicate that the datasets can be used to parameterize detailed residence time models in further work, and that sampling at higher than weekly frequency is needed to characterize quickflow. These results may be applicable to other mountainous tropical settings where soils, rainfall and isotopic composition patterns are similar. Many tropical regions are facing the challenge of meeting the water resource needs of an expanding population as potential climatic change may shift the balance between groundwater recharge and quickflow runoff, and may lead to greater flow extremes. This combined isotopic and solute chemistry approach holds promise for elucidating shifts in water sources with shifts in climate.

Please cite this article in press as: Scholl, M.A., et al. Stable-isotope and solute-chemistry approaches to flow characterization in a forested tropical watershed, Luquillo Mountains, Puerto Rico. Appl. Geochem. (2015), http://dx.doi.org/10.1016/j.apgeochem.2015.03.008

Appendix 1

(a) Stable isotope and solute chemistry data for eastern Puerto Rico in the Rio Mameyes watershed and other sites discussed in the text.

ID	Site name	Sample date	Type	δ^2H (‰)	$\delta^{18}O$ (‰)	*d*-excess (‰)	Ca (μeq l^{-1})	Mg (μeq l^{-1})	Sr (μeq)	SiO_2 (μmol)	Na (μeq l^{-1})	K (μeq l^{-1})	HCO_3 (μeq l^{-1})	Cl (μeq l^{-1})	SO_4 (μeq l^{-1})	NO_3 (μeq l^{-1})
LQS11-1	Rio Mameyes at Mameyes gage	2/10/2006	str	−4.5	−2.35	14.3	676	248	2.1	348	373	24	933	291	84	14.2
LQS9-1	Rio Mameyes above Q. Tabonuco	2/10/2006	str	−5.2	−2.49	14.7	563	177	1.6	338	336	18	747	250	79	6.1
LQS10-1	Quebrada Tabonuco	2/10/2006	str	−4.3	−2.15	12.9	1138	501	3.0	442	718	21	1806	440	104	<3.2
LQS8-1	Rio Mameyes at Rte. 990 crossing	2/10/2006	str	−6.0	−2.47	13.8	511	164	1.6	344	308	18	683	234	76	6.9
LQS7-1	Rio Mameyes nr. Sabana gage	2/10/2006	str	−5.3	−2.58	15.3	408	151	1.1	345	296	17	564	222	74	7.3
LQS12-1	Rio de la Mina above falls	2/11/2006	str	−4.8	−2.52	15.4	527	147	1.6	366	261	17	679	212	65	4.2
LQS1-1	Mameyes headwaters	2/9/2006	str	−4.9	−2.69	16.6	40	44	<0.5	124	195	9	87	168	43	3.2
LQS13-1	Mt. Britton trib. to Rio de la Mina	2/11/2006	str	−4.2	−2.58	16.4	93	71	<0.5	143	225	14	125	232	34	7.4
LQS11-2	Rio Mameyes at Mameyes gage	11/4/2006	str	−6.1	−2.5	13.9	599	202	1.6	304	257	15	810	226	73	10.5
LQS9-2	Rio Mameyes above Q. Tabonuco	11/4/2006	str	−7.2	−2.54	13.1	497	151	1.4	291	244	15	646	198	69	8.7
LQS10-2	Quebrada Tabonuco	11/4/2006	str	−6.1	−2.32	12.5	1043	476	2.7	452	544	18	1596	403	84	18.4
LQS8-2	Rio Mameyes at Rte. 990 crossing	11/4/2006	str	−6.9	−2.54	13.5	455	141	1.1	295	238	15	583	192	71	8.2
LQS7-2	Rio Mameyes nr. Sabana gage	11/4/2006	str	−7.6	−2.62	13.4	368	136	0.9	296	231	17	515	184	68	8.9
LQS12-2	Rio de la Mina above falls	11/4/2006	str	−6.4	−2.71	15.3	480	129	1.1	308	188	13	608	169	60	8.5
LQS1-2	Mameyes headwaters	11/7/2006	str	−6.7	−2.68	14.8	44	50	<0.5	165	188	11	111	146	41	5.3
LQS13-2	Mt. Britton trib. to Rio de la Mina	11/4/2006	str	−5.6	−2.66	15.7	127	78	0.5	75	186	10	175	187	42	8.5
LQS11-3	Rio Mameyes at Mameyes gage	9/29/2007	str	−5.2	−2.37	13.8	604	212	1.4	302	305	28	803	234	89	8.2
LQS9-3	Rio Mameyes above Q. Tabonuco	9/29/2007	str	−4.9	−2.4	14.3	445	144	1.1	273	252	16	585	190	77	4.4
LQS10-3	Quebrada Tabonuco	9/29/2007	str	−5.0	−2.14	12.1	1108	500	2.7	466	592	19	1614	418	116	12.3
LQS8-3	Rio Mameyes at Rte. 990 crossing	9/28/2007	str	−5.2	−2.58	15.5	301	108	0.8	219	225	15	416	159	59	4.0
LQS7-3	Rio Mameyes nr. Sabana gage	9/29/2007	str	−4.7	−2.43	14.7	358	127	0.9	285	240	15	480	177	72	4.7
LQS12-3	Rio de la Mina above falls	9/29/2007	str	−5.0	−2.52	15.1	499	137	1.2	330	218	15	624	166	63	4.0
LQS1-3	Mameyes headwaters	9/29/2007	str	−5.9	−2.58	14.8	40	47	<0.1	142	166	6	89	141	31	1.8
LQS13-3	Mt. Britton trib. to Rio de la Mina	9/28/2007	str	−6.5	−2.61	14.4	71	58	0.3	74	147	13	70	130	47	3.2
LQS11-4	Rio Mameyes at Mameyes gage	6/25/2008	str	−3.6	−2.02	12.5	744	260	1.9	356	368	26	952	299	96	6.5
LQS12-4	Rio de la Mina above falls	6/24/2008	str	−3.3	−1.94	12.3	241	109	0.7	244	229	15	297	236	53	4.7
LQS13-4	Mt. Britton trib. to Rio de la Mina	6/24/2008	str	−2.9	−2	13.1	110	86	0.4	129	214	16	108	264	49	3.1
LQS7-4	Rio Mameyes nr. Sabana gage	6/25/2008	str	−3.7	−2.28	14.6	442	162	1.2	367	288	18	600	229	79	4.2
LQS11-5	Rio Mameyes at Mameyes gage	1/10/2010	str	−2.9	−2.24	15.0										
LQS9-5	Rio Mameyes above Q. Tabonuco	1/10/2010	str	−3.6	−2.37	15.4										
LQS7-5	Rio Mameyes nr. Sabana gage	1/9/2010	str	−2.3	−2.44	17.2										
LQS12-5	Rio de la Mina above falls	1/10/2010	str	−3.5	−2.46	16.2										
LQS13-5	Mt. Britton trib. to Rio de la Mina	1/9/2010	str	−1.6	−2.29	16.8										
LQGW16	Caimitillo well (EYNF)	6/21/11	gw	−10.1	−2.9	13.1	1946	272	4.6	627	298	28	2083	224	252	
LQGW19	Palo Colorado well (EYNF)	6/21/11	gw	−6.5	−2.8	15.9	973	213	0.8	708	253	31	661	175	616	
LQGW16	Caimitillo well (EYNF)	5/29/12	gw	−6.0	−2.7	15.6	1961	288	4.5	638	294	24	2138	222	298	
LQGW19	Palo Colorado well (EYNF)	5/29/12	gw	−6.5	−2.72	15.3	819	188	0.8	668	217	23	598	174	503	
LQGW21	Aviary well (EYNF)	5/29/12	gw	−4.5	−2.33	14.1	1327	816	1.6	758	644	7	2390	370	95	
EV	El Verde Research Station, IITF, G	LTA	ppt	–	–	–	22	28			101	5		114	29	
BIS	BIS (Bisley lower tower) G,S	LTA, VWA	ppt	−9.5	−2.87	13.3	26	35			129	6		144	30	
PDE	Pico del Este (East Peak) G,S	LTA, VWA	ppt	−14.0	−3.77	15.2	39	41			158	12		172	43	
PDE	Pico del Este (East Peak) G,S	LTA, VWA	cw	−1.0	−2.12	15.0	96	107			532	31		618	152	
MPR	Rio Mameyes at Puente Roto S	VWA	ppt	−6.3	−2.32	11.9										
MP	Mameyes/Platanos site S	VWA	ppt	−8.6	−2.52	11.3										

Abbreviations: str = stream, gw = groundwater, ppt = rainfall, cw = cloud water, LTA = long term average, VWA = volume-weighted average, EYNF = El Yunque National Forest, G = chemistry data from Gioda et al. (2013), S = isotope data from Scholl et al. (2014).

(b) Location information for sample sites in eastern Puerto Rico.

Site ID	Map ID	Site name	Longitude (°W)	Latitude (°N)	Elevation, (m asl)	Well total depth and intake depth, (m bls)
LQS11	RMM	Rio Mameyes at Mameyes USGS gage 50066000	18.37226	−65.76311	5	–
LQS9	RMQT	Rio Mameyes above Q. Tabonuco	18.35966	−65.76887	11	–
LQS10	QT	Quebrada Tabonuco	18.35973	−65.76937	12	–
LQS8	RM990	Rio Mameyes at Rte. 990 crossing	18.34246	−65.75427	47	–
LQS7	MPR	Rio Mameyes nr. Sabana USGS gage 50065500 (Puente Roto)	18.32944	−65.75111	84	–
LQS12	RMF	Rio de la Mina above falls	18.30295	−65.77805	536	–
LQS1	RMH	Rio Mameyes headwaters	18.29592	−65.78941	732	–
LQS13	MBT	Mt. Britton tributary to Rio de la Mina	18.29845	−65.79199	778	–
LQGW16	LQGW16	Caimitillo well (GW16)	18.3008	−65.7856	645	102, 93
LQGW19	LQGW19	Palo Colorado well (GW19)	18.3006	−65.7875	694	107, 93
LQGW21	LQGW21	Aviary well (GW21)	18.3336	−65.7742	461	160, 148
EV	EV	El Verde Research Station, IITF, G	18.3239	−65.8175	380	–
BIS	BIS	Bisley lower tower, G,S			361	–
PDE	PDE	Pico del Este (East Peak) G,S	18.26975	−65.7596	1051	–
MP	MP	Mameyes/Platanos site S	18.3761	−65.7333	5	–

Abbreviations: asl = above sea level; bls = below land surface; G = chemistry data from Gioda et al. (2013); S = isotope data from Scholl et al. (2014).

Acknowledgements

This work was supported by the USGS Climate and Land Use Change Program, and the NSF Critical Zone Observatories Program Grant NSF EAR-0722476. Carlos Estrada (USFS) and Manuel Rosario and Angel Torres (USGS) helped with field work. We thank Haiping Qi, Jennifer Lorenz and Lauren Tarbox of the USGS Reston Stable Isotope Laboratory for analysis of isotope samples. Michael Doughten, Peggy Widman and Brett Uhle of the USGS analyzed solute chemistry for the contemporaneous sample sets. We thank Bill McDowell and Jody Potter, UNH, for the chemical analyses of the hydrograph separation samples. Comments from M. Alisa Mast of the USGS, and two anonymous reviewers improved this manuscript substantially. Any use of trade, product, or firm names is for descriptive purposes only and does not imply endorsement by the U.S. Government.

References

Bawiec, W.J., 1998. Geology, Geochemistry, Geophysics, Mineral Occurrences, and Mineral Resource Assessment for the Commonwealth of Puerto Rico: U.S. Geological Survey Open-File Report 98-38.

Beck, H.E., Bruijnzeel, L.A., van Dijk, A.I.J.M., McVicar, T.R., Scatena, F.N., Schellekens, J., 2013. The impact of forest regeneration on streamflow in 12 mesoscale humid tropical catchments. Hydrol. Earth Syst. Sci. 17, 2613–2635. http://dx.doi.org/10.5194/hess-17-2613-2013.

Bhatt, M.P., McDowell, W.H., 2007. Controls on major solutes within the drainage network of a rapidly weathering tropical watershed. Water Resour. Res. 43, W11402. http://dx.doi.org/10.1029/2007WR005915.

Bonell, M., 2005. Runoff generation in tropical forests. In: Bonell, M., Bruijnzeel, L.A. (Eds.), Forests, Water and People in the Humid Tropics: Past, Present and Future Hydrological Research for Integrated Land and Water Management. International Hydrology Series. Cambridge University Press, Cambridge, UK, pp. 314–406.

Bonell, M., Barnes, C.J., Grant, C.R., Howard, A., Burns, J., 1998. High rainfall, response-dominated catchments: a comparative study of experiments in tropical northeast Queensland with temperate New Zealand. In: Kendall, C., McDonnell, J.J. (Eds.), Isotope Tracers in Catchment Hydrology. Elsevier, Amsterdam, pp. 347–390.

Brocard, G.Y., Willenbring, J.K., Scatena, F.N., Johnson, A.H., submitted for publication. Knickpoint control on mass export and soil mineralogy in the Luquillo Mountains of Puerto Rico. Appl. Geochem., this issue.

Bruijnzeel, L.A., 2004. Hydrological functions of tropical forests: not seeing the soil for the trees? Agric. Ecosyst. Environ. 104 (1), 185–228.

Bruijnzeel, L.A., Bonell, M., Gilmour, D.A., Lamb, D., 2005. Forests, water and people in the humid tropics: an emerging view. In: Bonell, M., Bruijnzeel, L.A. (Eds.), Forests, Water and People in the Humid Tropics. International Hydrology Series. Cambridge University Press, Cambridge, UK, pp. 906–925.

Burns, D.A. et al., 2001. Quantifying contributions to storm runoff through end-member mixing analysis and hydrologic measurements at the Panola Mountain Research Watershed (Georgia, USA). Hydrol. Process. 15, 1903–1924. http://dx.doi.org/10.1002/hyp.246.

Buss, H.L., Brantley, S.L., Scatena, F.N., Bazilievskaya, E.A., Blum, A., Schulz, M., Jimenez, R., White, A.F., Rother, G., Cole, D., 2013. Probing the deep critical zone beneath the Luquillo Experimental Forest, Puerto Rico. Earth Surf. Proc. Land. 38 (10), 1170–1186. http://dx.doi.org/10.1002/esp.3409.

Buttle, J.M., McDonnell, J.J., 2005. Isotope tracers in catchment hydrology in the humid tropics. In: Bonell, M., Bruijnzeel, L.A. (Eds.), Forests, Water and People in the Humid Tropics. UNESCO International Hydrology Series. Cambridge University Press, Cambridge, UK, pp. 770–789.

Craig, H., 1961. Isotopic variations in meteoric waters. Science 133 (3465), 1702–1703. http://dx.doi.org/10.1126/science.133.3465.1702.

Crook, K.E., Scatena, F.N., Pringle, C.M., 2007. Water withdrawn from the Luquillo Experimental Forest, 2004. Gen. Tech. Report HTF-GTR-34. U.S. Department of Agriculture, Forest Service, International Institute of Tropical Forestry, San Juan, PR, 26 pp.

Dansgaard, W., 1964. Stable isotopes in precipitation. Tellus 16 (4), 436–468.

Dawson, T.E., Simonin, K.A., 2011. The roles of stable isotopes in forest hydrology and biogeochemistry. In: Levia, D.F., Carlyle-Moses, D.C., Tanaka, T. (Eds.), Forest Hydrology and Biogeochemistry: Synthesis of Past Research and Future Directions. Springer, New York, NY, pp. 137–161.

Elsenbeer, H., 2001. Hydrologic flowpaths in tropical rainforest soilscapes – a review. Hydrol. Process. 15, 1751–1759. http://dx.doi.org/10.1002/hyp.237.

Elsenbeer, H., Lorieri, D., Bonell, M., 1995. Mixing model approaches to estimate storm flow sources in an overland flow-dominated tropical rain forest catchment. Water Resour. Res. 31 (9), 2267–2278. http://dx.doi.org/10.1029/95WR01651.

Gat, J.R., Bowser, C.J., Kendall, C., 1994. The contribution of evaporation from the Great Lakes to the continental atmosphere: estimate based on stable isotope data. Geophys. Res. Lett. 21 (7), 557–560.

Gioda, A., Mayol-Bracero, O., Scatena, F.N., Weathers, K.C., Mateus, V.L., McDowell, W.H., 2013. Chemical constituents in clouds and rainwater in the Puerto Rican rainforest: potential sources and seasonal drivers. Atmos. Environ. 68, 208–220. http://dx.doi.org/10.1016/j.atmosenv.2012.11.017.

Godsey, S.E., Kirchner, J.W., Clow, D.W., 2009. Concentration–discharge relationships reflect chemostatic characteristics of US catchments. Hydrol. Process. 23 (13), 1844–1864. http://dx.doi.org/10.1002/hyp.7315.

Goller, R., Wilcke, W., Leng, M.J., Tobschall, H.J., Wagner, K., Valarezo, C., Zech, W., 2005. Tracing water paths through small catchments under a tropical montane rain forest in south Ecuador by an oxygen isotope approach. J. Hydrol. 308, 67–80. http://dx.doi.org/10.1016/j.jhydrol.2004.10.022.

Harman, C.J., 2015. Time-variable transit time distributions and transport: theory and application to storage-dependent transport of chloride in a watershed. Water Resour. Res. 51. http://dx.doi.org/10.1002/2014WR015707.

Heartsill-Scalley, T., Scatena, F.N., Estrada, C., McDowell, W.H., Lugo, A.E., 2007. Disturbance and long-term patterns of rainfall and throughfall nutrient fluxes in a subtropical wet forest in Puerto Rico. J. Hydrol. 333, 472–485. http://dx.doi.org/10.1016/j.jhydrol.2006.09.019.

Kabeya, N., Katsuyama, M., Kawasaki, M., Ohte, N., Sugimoto, A., 2007. Estimation of mean residence times of subsurface waters using seasonal variation in deuterium excess in a small headwater catchment in Japan. Hydrol. Process. 21 (3), 308–322. http://dx.doi.org/10.1002/hyp.6231.

Klaus, J., McDonnell, J.J., 2013. Hydrograph separation using stable isotopes: review and evaluation. J. Hydrol. 505, 47–64. http://dx.doi.org/10.1016/j.jhydrol.2013.09.006.

Krishnaswamy, J., Bonell, M., Venkatesh, B., Purandura, B.K., Rakesh, K.N., Lele, S., Kiran, M.C., Reddy, V., Badiger, S., 2013. The groundwater recharge response and hydrologic services of tropical humid forest ecosystems to use and reforestation: support for the "infiltration-evapotranspiration trade-off hypothesis". J. Hydrol. 498, 191–209. http://dx.doi.org/10.1016/j.hydrol.2013.06.034.

Kurtz, A.C., Lugolobi, F., Salvucci, G., 2011. Germanium-silicon as a flow path tracer: application to the Río Icacos watershed. Water Resour. Res. 47, W06516. http://dx.doi.org/10.1029/2010wr009853.

Lewis, S.C., LeGrande, A.N., Kelley, M., Schmidt, G.A., 2013. Modeling insights into deuterium excess as an indicator of water vapor source conditions. J. Geophys. Res.: Atmos. 118, 243–262. http://dx.doi.org/10.1029/2012JD017804.

Litt, G.F., Gardner, C.B., Ogden, F.L., Lyons, W.B., this issue. Hydrologic tracers and thresholds: a comparison of geochemical techniques for event-based stream hydrograph separation across multiple land covers in the Panama Canal Watershed. Appl. Geochem.

Lyon, S.W., Desilets, S.L.E., Troch, P.A., 2009. A tale of two isotopes: differences in hydrograph separation for a runoff event when using δD versus δ18O. Hydrol. Process. 23, 2095–2101. http://dx.doi.org/10.1002/hyp.7326.

McDowell, W.H., Asbury, C.E., 1994. Export of carbon, nitrogen and major ions from three tropical montane watersheds. Limnol. Oceanogr. 39 (1), 111–125.

Merlivat, L., Jouzel, J., 1979. Global climatic interpretation of the deuterium-oxygen 18 relationship for precipitation. J. Geophys. Res. 84 (C8), 5029–5033.

Muñoz-Villers, L., McDonnell, J.J., 2012. Runoff generation in a steep, tropical montane cloud forest catchment on permeable volcanic substrate. Water Resour. Res. 48, W09528. http://dx.doi.org/10.1029/2011WR011316.

Muñoz-Villers, L.E., McDonnell, J.J., 2013. Land use change effects on runoff generation in a humid tropical montane cloud forest region. Hydrol. Earth Syst. Sci. 17, 3543–3560. http://dx.doi.org/10.5194/hess-17-3543-2013.

Murphy, S.F., Stallard, R.F., 2012a. Water Quality and Landscape Processes of Four Watersheds in Eastern Puerto Rico. U.S. Geological Survey Professional Paper 1789. U.S. Geological Survey, 292 pp.

Murphy, S.F., Stallard, R.F., 2012b. Hydrology and climate of four watersheds in eastern Puerto Rico. In: Murphy, S.F., Stallard, R.F. (Eds.), Water Quality and Landscape Processes of Four Watersheds in Eastern Puerto Rico. U.S. Geological Survey Professional Paper 1789, pp. 43–84.

Murphy, S.F., Brantley, S.L., Blum, A., White, A.F., Dong, H., 1998. Chemical weathering in a tropical mountain watershed, Luquillo Mountains, Puerto Rico II – the rate and mechanism of biotite weathering. Geochim. Cosmochim. Acta 62 (2), 227–243.

Murphy, S.F., Stallard, R.F., Larsen, M.C., Gould, W.A., 2012. Physiography, geology, and land cover of four watersheds in Eastern Puerto Rico. In: Murphy, S.F., Stallard, R.F. (Eds.), Water Quality and Landscape Processes of Four Watersheds in Eastern Puerto Rico. U.S. Geological Survey Professional Paper 1789, pp. 5–20.

Ogden, F.L., Harmon, R.S., 2012. Editorial: special issue of J. Hydrology on Tropical Hydrology. J. Hydrol. 462–463, 1–3. http://dx.doi.org/10.1016/j.jhydrol.2012.07.017.

Ogden, F.L., Crouch, T.D., Stallard, R.F., Hall, J.S., 2013. Effect of land cover and use on dry season river runoff, runoff efficiency, and peak storm runoff in the seasonal tropics of Central Panama. Water Resour. Res. 49, 1–20. http://dx.doi.org/10.1002/2013WR013956.

Pike, A.S., Scatena, F.N., Wohl, E.E., 2010. Lithological and fluvial controls on the geomorphology of tropical montane stream channels in Puerto Rico. Earth Surf. Proc. Land. 35 (12), 1402–1417. http://dx.doi.org/10.1002/esp.1978.

Révész, K., Coplen, T.B., 2008a. Determination of the delta ($^{2}H/^{1}H$) of water: RSIL lab code 1574. In: Revesz, K., Coplen, T.B. (Eds.), Methods of the Reston Stable Isotope Laboratory. U.S. Geological Survey Techniques and Methods 10-C1, 27 p.

Révész, K., Coplen, T.B., 2008b. Determination of the delta ($^{18}O/^{16}O$) of water: RSIL lab code 489. In: Revesz, K., Coplen, T.B. (Eds.), Methods of the Reston Stable Isotope Laboratory. U.S. Geological Survey Techniques and Methods 10-C2, 28 p.

Rivera-Ramirez, H.D., Warner, G.S., Scatena, F.N., 2002. Prediction of master recession curves and baseflow recessions in the Luquillo Mountains of Puerto Rico. J. Am. Water Resour. Assoc. 38 (3), 693–704.

Salati, E., Dall'Olio, A., Matsui, E., Gat, J.R., 1979. Recycling of water in the Amazon Basin: an isotopic study. Water Resour. Res. 15 (5), 1250–1258.

Schellekens, J., Scatena, F.N., Bruijnzeel, L.A., Wickel, A.J., 1999. Modelling rainfall interception by a lowland tropical rain forest in northeastern Puerto Rico. J. Hydrol. 225 (3–4), 168–184.

Schellekens, J., Scatena, F.N., Bruijnzeel, L.A., van Dijk, A.I.J.M., Groen, M.M.A., van Hogezand, R.J.P., 2004. Stormflow generation in a small rainforest catchment in the Luquillo Experimental Forest, Puerto Rico. Hydrol. Process. 18, 505–530. http://dx.doi.org/10.1002/hyp.1335.

Scholl, M.A., Murphy, S.F., 2014. Precipitation isotopes link regional climate patterns to water supply in a tropical mountain forest, eastern Puerto Rico. Water Resour. Res. 50 (5). http://dx.doi.org/10.1002/2013WR014413.

Scholl, M.A., Gingerich, S.B., Tribble, G.W., 2002. The influence of microclimates and fog on stable isotope signatures used in interpretation of regional hydrology: East Maui, Hawaii. J. Hydrol. 264, 170–184.

Scholl, M.A., Shanley, J.B., Zegarra, J.P., Coplen, T.B., 2009. The stable isotope amount effect: new insights from NEXRAD echo tops, Luquillo Mountains, Puerto Rico. Water Resour. Res. 45, W12407. http://dx.doi.org/10.1029/2008WR007515.

Scholl, M.A., Torres-Sanchez, A., Rosario-Torres, M., 2014. Stable Isotope ($\delta^{18}O$ and $\delta^{2}H$) Data for Precipitation, Stream Water, and Groundwater in Puerto Rico. USGS Open File Report 2014-1101, Reston, VA, 26 p.

Seiders, Victor M., 1971. Geologic Map of the El Yunque Quadrangle, Puerto Rico, U.S. Geological Survey Miscellaneous Geologic Investigations Map I-658.

Shanley, J.B., McDowell, W.H., Stallard, R.F., 2011. Long-term patterns and short-term dynamics of stream solutes and suspended sediment in a rapidly weathering tropical watershed. Water Resour. Res. 47, W07515. http://dx.doi.org/10.1029/2010WR009788.

Siegenthaler, U., Oeschger, H., 1980. Correlation of 18O in precipitation with temperature and altitude. Nature 285, 314–317.

Simonin, K.A., Link, P., Rempe, D., Miller, S., Oshun, J., Bode, C., Dietrich, W.E., Fung, I., Dawson, T.E., 2013. Vegetation induced changes in the stable isotope composition of near surface humidity. Ecohydrology 7 (3), 936–949. http://dx.doi.org/10.1002/eco.1420.

Stallard, R.F., Murphy, S.F., 2012. Water quality and mass transport in four watersheds in Eastern Puerto Rico. In: Murphy, S.F., Stallard, R.F. (Eds.), Water Quality and Landscape Processes of Four Watersheds in Eastern Puerto Rico. U.S. Geological Survey Professional Paper 1789, pp. 113–152.

Stallard, R.F., Murphy, S.F., 2014. A unified assessment of hydrologic and biogeochemical responses in research watersheds in eastern Puerto Rico using runoff–concentration relations. Aquat. Geochem. 20 (2–3), 115–139. http://dx.doi.org/10.1007/s10498-013-9216-5.

Timbe, E., Windhorst, D., Crespo, P., Frede, H.-G., Feyen, J., Breuer, L., 2014. Understanding uncertainties when inferring mean transit times of water through tracer-based lumped-parameter models in Andean tropical montane cloud forest catchments. Hydrol. Earth Syst. Sci. 18, 1503–1523. http://dx.doi.org/10.5194/hess-18-1503-2014.

Van Beusekom, A.E., Gonzalez, G., Rivera, M.M., 2015. Short-term precipitation and temperature trends along an elevation gradient in Northeastern Puerto Rico. Earth Interact. 19 (3), 1–33. http://dx.doi.org/10.1175/EI-D-14-0023.1.

Weiler, M., McGlynn, B.L., McGuire, K.J., McDonnell, J.J., 2003. How does rainfall become runoff? A combined tracer and runoff transfer function approach. Water Resour. Res. 39 (11), 1315. http://dx.doi.org/10.1029/2003WR00233.

White, A.F., Blum, A., Schulz, M.S., Vivit, D., Stonestrom, D.A., Larsen, M.C., Murphy, S.F., Eberl, D.D., 1998. Chemical weathering in a tropical mountain watershed, Luquillo Mountains, Puerto Rico I – weathering rates based on mineral and solute mass balances. Geochim. Cosmochim. Acta 62 (2), 209–226.

Wohl, E. et al., 2012. The hydrology of the humid tropics. Nat. Clim. Change 2, 655–662. http://dx.doi.org/10.1038/NCLIMATE1556.

Yi-Balan, S.A., Amundson, R., Buss, H.L., 2014. Decoupling of sulfur and nitrogen cycling due to biotic processes in a tropical rainforest. Geochim. Cosmochim. Acta 142, 411–428. http://dx.doi.org/10.1016/j.gca.2014.05.049.

Please cite this article in press as: Scholl, M.A., et al. Stable-isotope and solute-chemistry approaches to flow characterization in a forested tropical watershed, Luquillo Mountains, Puerto Rico. Appl. Geochem. (2015), http://dx.doi.org/10.1016/j.apgeochem.2015.03.008